

# RELAXATION AND DECOHERENCE: WHAT'S NEW?

RALPH v. BALTZ

*Institut für Theorie der Kondensierten Materie*

*Universität Karlsruhe, D-76128 Karlsruhe, Germany* \*

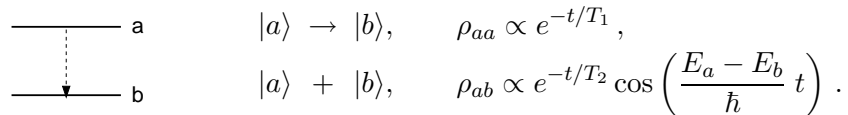
## 1. Introduction

Relaxation and decoherence are omnipresent phenomena in macro-physics

- *Relaxation*: evolution of an initial state towards a steady state.
- *Decoherence*: decay of correlation  $G(t, t') = \langle x(t)x(t') \rangle \rightarrow 0$  with time  $|t - t'| \rightarrow \infty$ .  $x(t)$  can be any classical quantity or quantum observable which permits the linear superposition (i.e.  $x$  has a “phase”).

Some examples are sketched in Fig. 1. For fields, like the electrical field  $\mathcal{E}(\mathbf{r}, t)$  of a light wave, one may discuss relaxation and correlation for different space-time points which is called temporal and spatial coherence.

The microscopic origin of relaxation and decoherence is *irreversibility*, i.e., the coupling of a *system* to its environment by which a *pure state* is transformed into a *mixed state*. For instance, a two-level-system (like a spin 1/2 in a magnetic field or an atom under near resonant excitation)  $\hat{\rho}$  is a  $2 \times 2$ -matrix.


$$\begin{array}{l} \text{---} \quad \text{a} \\ \vdots \\ \text{---} \quad \text{b} \end{array} \quad \begin{array}{l} |a\rangle \rightarrow |b\rangle, \\ |a\rangle + |b\rangle, \end{array} \quad \begin{array}{l} \rho_{aa} \propto e^{-t/T_1}, \\ \rho_{ab} \propto e^{-t/T_2} \cos\left(\frac{E_a - E_b}{\hbar} t\right). \end{array}$$

The diagonal elements  $\rho_{aa} \geq 0$  and  $\rho_{bb} = 1 - \rho_{aa} \geq 0$  give the populations of the levels, whereas the nondiagonal elements  $\rho_{ba} = \rho_{ab}^*$  describe the coherent motion, i.e. an oscillating (electrical or magnetic) dipole moment. In simple cases relaxation and coherence can be characterized by two different relaxation times which are usually denoted by  $T_1$  (diagonal elements) and  $T_2$  (nondiagonal elements),  $T_2 \leq 2T_1$ .

---

\* <http://www.tkm.uni-karlsruhe.de/personal/baltz/>

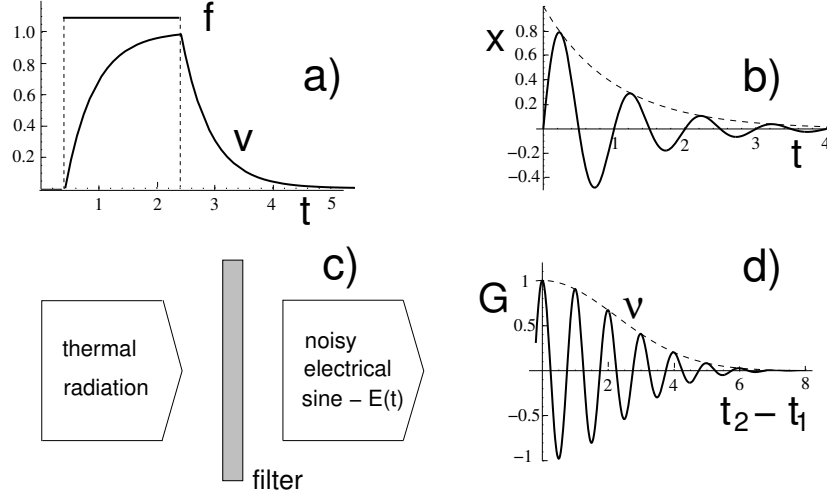


*Figure 1.* Upper panel: time dependence of two classical relaxing systems: (a) Particle in a viscous fluid subjected to an external force  $f(t)$ , (b) harmonic oscillator. Lower Panel: (c) filtered thermal light, (d) correlation function ( $\mathcal{V}$ : fringe contrast in an interferometer).

This article provides an overview on typical relaxation and decoherence phenomena in classical and quantum systems, see also some previous Erice contributions[1]. In addition, various examples are given including optically generated exciton spin states in quantum dots which are currently of interest in spintronics[2]. Decoherence is also an important issue in connection with the appearance of a classical world in quantum theory and the quantum measurement problem.

## 2. Relaxation in Classical Systems

In the following we denote the relaxing quantity by “ $v$ ” which may be also a dipole moment or position etc.

### 2.1. GENERAL PROPERTIES OF LINEAR RELAXING SYSTEMS

The prototype of relaxation is characterized by an exponential decay,  $v(t) \propto \exp(-\gamma t)$ , which is termed *Debye-relaxation*.  $\gamma$  is the relaxation rate and  $\tau = 1/\gamma$  is the relaxation time. Including an external “force”  $f(t)$  of arbitrary time-dependence, Debye-relaxation obeys a first order differential equation whose solution can be given in terms of its *Green-function*  $\chi_D(t)$

$$\dot{v}(t) + \gamma v(t) = f(t), \quad (1)$$

$$v(t) = \int_{-\infty}^{\infty} \chi_D(t-t') f(t') dt', \quad (2)$$

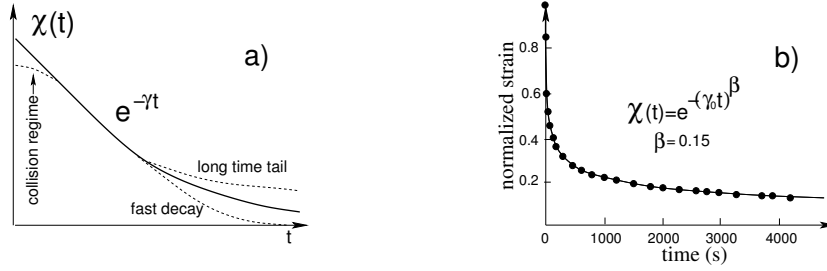


Figure 2. (a) Time dependence of typical (monotonous) relaxing processes. (b) Stretched exponential decay of strain recovery in polycarbonate[5].

$$\chi_D(t) = e^{-\gamma t} \Theta(t). \quad (3)$$

Instead of specifying an equation of motion for the relaxing quantity a *linear system* may be equally well characterized by an arbitrary causal function  $\chi(t)$  ( $\chi(t) \equiv 0, t < 0$ ) which – like a Green–function – gives the response with respect to a  $\delta(t)$ –pulse, see Fig. 2. As  $\chi(t)$  fully describes the input–output relationship (2) this function is also called *system function*.

In frequency–space<sup>1</sup> the convolution integral (2) becomes a product

$$v(t) = \int_{-\infty}^{\infty} v(\omega) e^{-i\omega t} \frac{d\omega}{2\pi}, \quad \text{etc.} \quad (4)$$

$$v(\omega) = \chi(\omega) f(\omega). \quad (5)$$

Due to causality, the *dynamical susceptibility*<sup>2</sup>

$$\chi(\omega) = \int_0^{\infty} \chi(t) e^{i\omega t} dt = \int_0^{\infty} \chi(t) e^{-\omega_i t} e^{i\omega_r t} dt \quad (6)$$

is an analytic function in the upper part of the *complex  $\omega$ –plane*. In  $\text{Im } \omega = \omega_i < 0$ , however,  $\chi(\omega)$  must have singularities (apart from the trivial case  $\chi(\omega) = \text{const}$ ). In terms of singularities, Debye–relaxation provides the simplest case: it has a first order pole at  $\omega = -i\gamma$ , see Fig. 3.

$$\chi_D(\omega) = \frac{1}{\gamma - i\omega} = \frac{\gamma}{\gamma^2 + \omega^2} + i \frac{\omega}{\gamma^2 + \omega^2}. \quad (7)$$

The real part of the susceptibility,  $\chi_1 = \text{Re } \chi$ , determines the cycle–averaged dissipated power whereas  $\chi_2 = \text{Im } \chi$  describes the flow of energy from the driving force to the system and vice versa (“dispersion”).

<sup>1</sup> Fouriertransformation is with  $\exp(-i\omega t)$  so that it conforms with the quantum mechanical time–dependence  $\exp(-iEt/\hbar)$ .

<sup>2</sup> The physical susceptibility may have in addition a prefactor depending on the relation between  $f(t)$  and the physical driving “force”, e.g.  $E(t)$ .

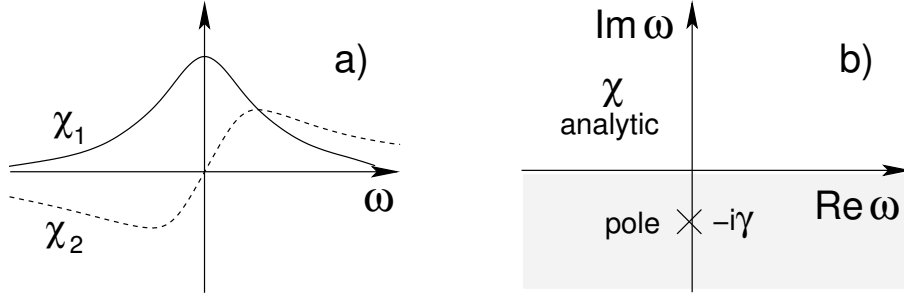


Figure 3. (a) Sketch of the real and imaginary parts of the Debye susceptibility. (b) Location of singularities of  $\chi(\omega)$  in the complex  $\omega$ -plane.

A characteristic property of Debye relaxation is the appearance of a semicircle when plotting the real/imaginary parts of  $\chi(\omega)$  on the horizontal/vertical axis with  $\omega$  as a parameter (Cole–Cole plot), see Fig. 4(a). Experimental data, however, are usually located below the semicircle. In many cases, the experimental results can be very well fitted by a “Cole–Cole function”,

$$\chi_{\text{CC}}(\omega) = \frac{1}{1 - (i\tau_0\omega)^{1-\alpha}}, \quad 0 \leq \alpha < 1. \quad (8)$$

Nevertheless, the benefit of such a fit is not obvious, see Fig. 4(b).

An often used generalization of (3) is a (statistical) distribution of relaxation rates in form of “parallel–relaxation”

$$\chi(t) = \int_0^\infty w(\gamma) e^{-\gamma t} d\gamma \Theta(t), \quad (9)$$

$$\int_0^\infty w(\gamma) d\gamma = 1, \quad w(\gamma) \geq 0. \quad (10)$$

$\chi(t)$  is the Laplace–transform of  $w(\gamma)$ .<sup>3</sup> Note,  $\dot{\chi}(t=0) = -\int \gamma w(\gamma) d\gamma < 0$  is the negative first moment of  $w(\gamma)$ . Within this model, the Cole–Cole plot is always under the Debye–semicircle.

## 2.2. EXAMPLES

### 2.2.1. Gaussian band of width $\Gamma$ centered at $\gamma_0$

$$w(\gamma) = \frac{1}{\sqrt{\pi}\Gamma} e^{-\frac{(\gamma-\gamma_0)^2}{\Gamma^2}}, \quad (11)$$

$$\chi(t) = \begin{cases} e^{-\gamma_0 t}, & \gamma_0 t \ll 1, \\ \frac{e^{-(\gamma_0/\Gamma)^2}}{\sqrt{\pi}\Gamma t}, & \gamma_0 t \gg 1. \end{cases} \quad (12)$$

<sup>3</sup> Equivalently, one may use a distribution function for the relaxation times  $\tilde{w}(\tau)$ .

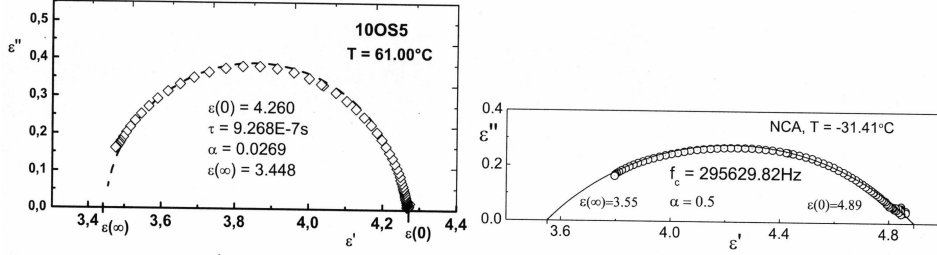


Figure 4. Relaxation of electrical dipoles in two different samples of liquid crystals,  $\epsilon(\omega) = \epsilon(\infty) + \chi(\omega)$ . (left) Almost pure Debye-type spectrum and (right) Cole-Cole relaxation. According to Haase and Wrobel[3].

### 2.2.2. Power-law decay

The following distribution (which has a broad maximum at  $\gamma_m = n/\tau_0$ ) leads to a power-law decay

$$w(\gamma) = \frac{\tau_0^{n+1}}{n!} \gamma^n e^{-\tau_0 \gamma}, \quad \chi(t) = \left[ \frac{\tau_0}{\tau_0 + t} \right]^{n+1}. \quad (13)$$

### 2.2.3. Stretched exponential

Relaxation in complex strongly interacting systems often follows a *stretched exponential* form[5], see also Fig. 2(b),

$$\chi(t) = e^{-(\gamma_0 t)^\beta}, \quad 0 < \beta \leq 1. \quad (14)$$

Kohlrausch[4] (p. 179) first suggested (14) to describe viscoelasticity but there are many examples (including transport and dielectric properties) which supports the stretched exponential as a universal law, see e.g., Refs. [6](a-c). As  $\dot{\chi}(t=0) = -\infty$  the corresponding distribution function  $w(\gamma)$  must either have a pathological tail  $w(\gamma) \rightarrow 1/\gamma^{2-\delta}$  ( $\delta > 0$ ) or (14) does not hold for  $t \rightarrow 0$ , see Fig. 2. The long time behaviour, on the other hand, corresponds to the strong decrease of  $w(\gamma)$  for small values of  $\gamma$ , i.e., large relaxation times.

An analytical example for the case  $\beta = 1/2$  in terms of parallel relaxation can be found in tables of Laplace-transforms[7](Vol. 5, Ch. 2.2)

$$\chi(t) = e^{-\sqrt{\gamma_0 t}} \Theta(t), \quad w(\gamma) = \sqrt{\frac{\gamma_0}{4\pi\gamma^3}} e^{-\frac{\gamma_0}{4\gamma}}. \quad (15)$$

$w(\gamma)$  has a broad maximum at  $\gamma_m = \gamma_0/6$ .

Very likely, the stretched exponential originates from many sequential dynamically correlated activation steps rather than from parallel relaxation[8].

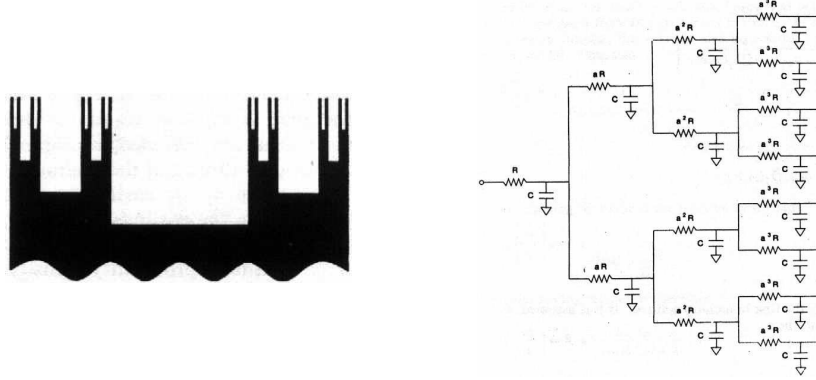


Figure 5. (left) Liu's Cantor block model of a rough interface between an electrolyte (black) and an electrode (white), two grooves, each with four stages of branching are shown. (right) Equivalent circuit. According to Liu[11](a).

#### 2.2.4. Frequency dependent relaxation rate

C-C-plots above the semicircle may arise in systems which either display

- “faster than exponential relaxation”, e.g.,  $\chi(t) = (1-\gamma t)^2 \Theta(t) \Theta(1-\gamma t)$ ,
- or have a frequency dependent relaxation rate with  $\gamma(\omega) \rightarrow 0$  for  $\omega \rightarrow \infty$  (“sequential relaxation”)

$$\chi(\omega) = \frac{1}{-i\omega + \gamma(\omega)}. \quad (16)$$

In the time domain, a frequency dependent  $\gamma(\omega)$  leads to relaxation with a memory

$$\dot{x}(t) + \int_{-\infty}^{\infty} \gamma(t-t') x(t') dt' = f(t), \quad (17)$$

where  $\gamma(t)$  is the Fourier-transform of  $\gamma(\omega)$ . Causality requires that  $\gamma(t) \equiv 0$  for  $t < 0$  so that  $\gamma(\omega)$  is an analytic function in  $\text{Im } \omega > 0$ .

A simple approximation for  $\gamma(\omega)$  is of “Drude” type

$$\gamma(\omega) = \gamma_D \frac{\gamma_c}{-i\omega + \gamma_c}. \quad (18)$$

$\gamma_c \geq \gamma_D$  may be interpreted as a “collision” rate. For this model  $\chi(\omega)$  displays two poles in  $\text{Im } \omega < 0$  and a zero in  $\text{Im } \omega > 0$ . For  $\gamma_D < \gamma_c < 4\gamma_D$ ,  $\chi(t)$  even shows oscillatory behaviour. For experimental evidence see, e.g., measurements by Dressel et al.[9]. Finally, we mention that fractional kinetics can be also formulated by the new and fancy mathematics of “fractional derivatives” [10].

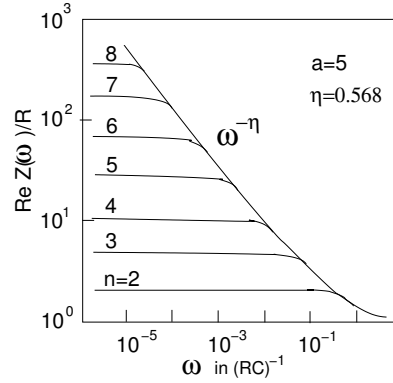


Figure 6. Frequency dependence of the real part of the impedance of the fractal network in Fig. 5 for finite and infinite stages. According to Liu[11](a).

### 2.3. IMPEDANCE OF A ROUGH SURFACE

An interesting example for sequential relaxation is the *Cantor-RC-circuit* model[11] which is supposed to describe the impedance of a rough (fractal) metal surface[12], see Fig. 5. The impedance of the network is given by the infinite continued fraction[11](b)

$$Z(\omega) = R + \frac{1}{j\omega C + \frac{2}{aR + \frac{1}{j\omega C + \dots}}} \quad (19)$$

which fulfills the exact scaling relation<sup>4</sup>

$$Z(\omega/a) = R + \frac{aZ(\omega)}{j\omega CZ(\omega) + 2}. \quad (20)$$

For  $\omega \rightarrow 0$  and  $a > 2$ , Eq. (20) becomes  $Z(\omega/a) = aZ(\omega)/2$  which implies  $Z(\omega) \propto \omega^{-\eta}$  with  $\eta = 1 - \ln(2)/\ln(a) = 1 - \bar{d}$ ,  $\bar{d}$  is the fractal dimension of the surface, see Fig. 6.

For  $a = 1$  (yet unphysical) (20) becomes a quadratic equation for  $Z$  which can be solved analytically. Limiting cases are

$$\omega \rightarrow 0 : Z_{a=1}(\omega) = 2R(1 - jRC\omega), \quad (21)$$

$$\omega \rightarrow \infty : Z_{a=1}(\omega) = R\left(1 + \frac{2}{(RC\omega)^2}\right) - \frac{j}{2\omega C}. \quad (22)$$

<sup>4</sup> Electrotechnical convention:  $j = -i$ , time dependence is by  $\exp(+j\omega t)$ .

### 3. Interaction of a Particle with a Bath

Many situations in nature can be adequately described by a system with one (or only a few) degrees of freedom (“particle”) in contact with a rather complex environment modelled by a reservoir of harmonic oscillators or a “bath” of temperature  $T$ . In the classical limit the interaction with the bath is described by a stochastic force acting on the particle

$$F_{\text{bath}} = -\eta v + F_{\text{st}}, \quad (23)$$

where  $-\eta v$  describes the slowly varying frictional contribution and  $F_{\text{st}}$  denotes a rapidly fluctuating force with zero mean  $\overline{F_{\text{st}}(t)} = 0$ . For a stationary Gaussian process, the statistical properties are fully characterized by its correlation function which in the case of an uncorrelated process reads

$$K_{\text{FF}}(t_1, t_2) = \overline{F_{\text{st}}(t + t_1)F_{\text{st}}(t + t_2)} = 2\eta k_{\text{B}}T\delta(t_2 - t_1). \quad (24)$$

The overline denotes a time average and the constant  $\eta (= M\gamma)$  is proportional to the viscosity.

The *Langevin equation*

$$M\ddot{q}(t) + \eta\dot{q}(t) + V'(q) = F_{\text{st}}(t) \quad (25)$$

describes, for example, a heavy Brownian particle of mass  $M$  immersed in a fluid of light particles and driven by an external force  $F = -V'(q)$ . Another example is Nyquist noise in a  $R$ – $L$  circuit ( $V \equiv 0$ ). For an overview see, e.g., Reif[13] (Sect. 15).

For a free particle (25) conforms with (1); the velocity–force and velocity–velocity correlation functions (in thermal equilibrium) follow from (2,3)

$$K_{\text{vF}}(t_1, t_2) = \overline{v(t + t_1)F_{\text{st}}(t + t_2)} = 2\eta k_{\text{B}}T \chi(t_1 - t_2), \quad (26)$$

$$K_{\text{vv}}(t_1, t_2) = \overline{v(t + t_1)v(t + t_2)} = \frac{k_{\text{B}}T}{M} e^{-\gamma|t_1 - t_2|}. \quad (27)$$

Eq. (27) includes the equipartition theorem  $\overline{Mv^2(t)}/2 = k_{\text{B}}T/2$ . Under the influence of the stochastic force the particle describes *Brownian motion*<sup>5</sup>

$$q(t) = \int_0^t v(t') dt', \quad (28)$$

$$\overline{q^2}(t) = \int_0^t \int_0^t K_{\text{vv}}(t', t'') dt' dt'' \rightarrow 2Dt, \quad (t \rightarrow \infty), \quad (29)$$

where  $D = \overline{v^2}/\gamma = k_{\text{B}}T/(M\gamma)$  is the diffusion coefficient.

<sup>5</sup> Note, one of Einstein’s three seminal 1905–papers was on diffusion[14].

As an example how to eliminate the reservoir variables explicitly, we consider a classical particle of mass  $M$  and coordinate  $q$ , which is bilinearly coupled to a system of uncoupled harmonic oscillators

$$H = H_s + H_{\text{res}} + H_{\text{int}}, \quad (30)$$

$$H_s = \frac{p^2}{2M} + V(q), \quad (31)$$

$$H_{\text{res}} = \sum_i \frac{p_i^2}{2m_i} + \frac{1}{2} m_i \omega_i^2 x_i^2, \quad (32)$$

$$H_{\text{int}} = -q \sum_i c_i x_i + q^2 \sum_i \frac{c_i^2}{2m_i \omega_i^2}, \quad (33)$$

with suitable constants for  $c_i, \omega_i, m_i$ . This model has been used by several authors and is nowadays known as the *Caldeira–Leggett model*[15]. For an elementary version see Ingold’s review article in Ref.[16] (p. 213).

The equations of motion of the coupled system are:

$$M\ddot{q} + V'(q) + q \sum_i \frac{c_i^2}{m_i \omega_i^2} = \sum_i c_i x_i, \quad (34)$$

$$\ddot{x}_i + \omega_i^2 x_i = \frac{c_i}{m_i} q(t). \quad (35)$$

As the reservoir represents a system of uncoupled oscillators (35) can be easily solved in terms of the appropriate Green–function

$$x_i(t) = x_i(0) \cos(\omega_i t) + \frac{p_i(0)}{m_i} \sin(\omega_i t) + \int_0^t \frac{c_i}{m_i \omega_i} \sin[\omega_i(t-t')] q(t') dt'. \quad (36)$$

Inserting (36) into (34) yields a closed equation for  $q(t)$

$$M\ddot{q}(t) + \int_0^t M\gamma(t-t') \dot{q}(t') dt' + V'(q) = \xi(t), \quad (37)$$

$$\gamma(t) = \frac{2}{\pi} \int_0^\infty \frac{J(\omega)}{\omega} \cos(\omega t) d\omega, \quad (38)$$

$$J(\omega) = \pi \sum_i \frac{c_i^2}{2M m_i \omega_i} \delta(\omega - \omega_i). \quad (39)$$

Comparison with (25) shows that the relaxation process acquired a memory described by  $\gamma(t-t')$ , i.e., a frequency dependent relaxation rate  $\gamma(\omega)$ , (non–Markovian process).  $\xi(t)$  is the microscopic representation of the fluctuating force  $F_{\text{st}}(t)$  which depends on the initial conditions of the reservoir variables and is not explicitly stated here.

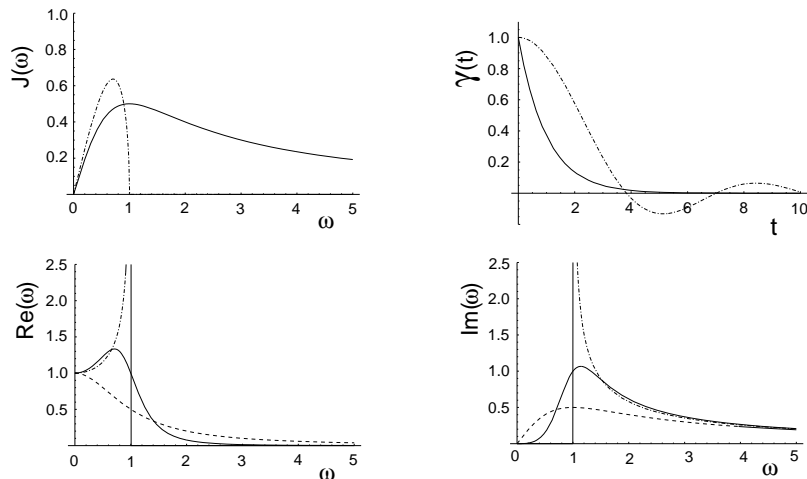


Figure 7. Upper panel: Spectral density of the reservoir oscillators (left) and memory functions (right). Solid lines: Caldeira–Leggett model with a Drude form, dashed lines: Drude–model, dashed dotted lines: Rubin model. (Dimensionless quantities,  $M_0/M = 1$ ). Lower panel: Real and imaginary parts of the electrical conductivity  $\sigma \propto \chi$ .

For a finite number of reservoir oscillators the total system will always return to its initial state after a finite (Poincaré) recurrence time or may come arbitrarily close to it. For  $N \rightarrow \infty$ , however, the Poincaré time becomes infinite, simulating dissipative behavior. We therefore first take the limit  $N \rightarrow \infty$  and consider the spectral density of reservoir modes  $J(\omega)$  as a continuous function. Frictional damping,  $\gamma(t) = \gamma_0 \delta(t)$ , is obtained for  $J(\omega) \propto \omega$ . A more realistic behavior would be a “Drude” function

$$J(\omega) = \gamma_0 \omega \frac{\gamma_D^2}{\omega^2 + \gamma_D^2}, \quad \gamma(t) = \gamma_0 \gamma_D e^{-\gamma_D t}, \quad (40)$$

which is linear for  $\omega \rightarrow 0$  but goes smoothly to zero for  $\omega \gg \gamma_D$ , see Fig. 7. Note, memory effects do not only lead to a frequency dependent scattering rate ( $= \text{Re} \gamma(\omega)$ ) but to a shift in the resonance frequency ( $= \text{Im} \gamma(\omega)$ ), too.

Another nontrivial yet exactly solvable model is obtained by a linear chain with one mass replaced by a particle of (arbitrary) mass  $M_0$  (Rubin–model). The left and right semi–infinite wings of the chain serve as a “reservoir” to which the central particle is coupled.

As a result the damping kernels are

$$\gamma(t) = \frac{M_0}{M} \omega_L \frac{J_1(\omega_L t)}{t}, \quad (41)$$

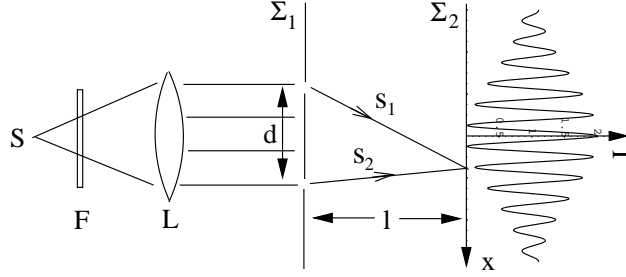


Figure 8. Arrangement of components for an idealized Young's interference experiment. Interferogram shown in the limit of infinitely small slits and  $\lambda \ll d \ll l$ . Gaussian spectral filter  $F$ .

$$\gamma(\omega) = \frac{M_0}{M} \begin{cases} \sqrt{\omega_L^2 - \omega^2} + i\omega, & |\omega| < \omega_L, \\ i \frac{\omega_L^2 \text{sgn}(\omega)}{\omega_L + \sqrt{\omega^2 - \omega_L^2}}, & |\omega| > \omega_L, \end{cases} \quad (42)$$

$$J(\omega) = \omega \frac{M_0}{M} \sqrt{\omega_L^2 - \omega^2} \Theta(\omega_L^2 - \omega^2). \quad (43)$$

$J_1(x)$  is a Bessel-function. For details see Fick and Sauermann book[17] (p. 255). In contrast to the "Drude case"  $\gamma(t)$  shows oscillations and decays merely algebraically for large times, see Fig. 7.

$$\gamma(t) \rightarrow \frac{M_0}{M} \sqrt{\frac{2\omega_L}{\pi}} \frac{\sin[\omega_L t - \pi/4]}{t^{3/2}}. \quad (44)$$

These oscillations reflect the upper cut-off in  $J(\omega)$  at the maximum phonon frequency  $\omega_L$ .

#### 4. Coherence in Classical Systems

The degree of coherence of a signal " $x(t)$ " or a field  $\mathcal{E}(\mathbf{r}, t)$  etc., is measured in terms of correlation at different times (or space-time points)

$$G(t, t') = \langle x(t)x(t') \rangle. \quad (45)$$

For stationary, ergodic ensembles, time- and ensemble averages give identical results. Moreover, the following general properties hold[13]

- $G(t, t') = G(t - t') = G(|t - t'|)$ ,
- $|G(t - t')| \leq G(0)$ ,
- $G(t) = \int_{-\infty}^{\infty} |x(\omega)|^2 e^{i\omega t} \frac{d\omega}{2\pi}$ , (Wiener-Khinchine theorem).

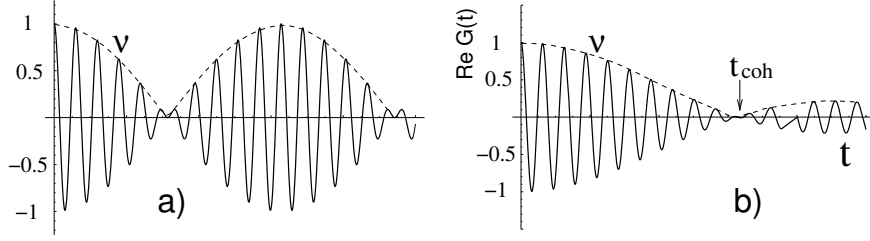


Figure 9. First order coherence functions as a function of time. (a) Two modes with  $\omega_j = (1 \pm 0.05)\omega_0$  and (b) many uncorrelated modes with a “box” spectrum centered at  $\omega_0$  and full width  $\Delta\omega = 0.1\omega_0$ .  $\mathcal{V}$  is the visibility of the fringes.

The prototype of a device to measure the optical coherence(-time) of light is the *Young double slit interference experiment*<sup>6</sup>, see Fig. 8. In the following discussion, we shall ignore complications arising from the finite source diameter and consequent lack of perfect parallelism in the illuminating beam, diffraction effects at the pinholes (or slits), reduction of amplitude with distances  $s_1, s_2$  etc., in order that attention be focused on the properties of the incident radiation rather than on details of the measuring device. Let  $\mathcal{E}(\mathbf{r}, t)$  be the electrical field of the radiation at point  $\mathbf{r}$  on the observation screen at time  $t$ . This field is a superposition of the incident field at the slits  $\mathbf{r}_1, \mathbf{r}_2$  at earlier times  $t_{1,2} = t - s_{1,2}/c$ ,

$$\mathcal{E}(\mathbf{r}, t) \propto \mathcal{E}^{\text{in}}(\mathbf{r}_1, t_1) + \mathcal{E}^{\text{in}}(\mathbf{r}_2, t_2). \quad (46)$$

As a result, the (cycle averaged) light intensity  $I \propto \overline{|\mathcal{E}(\mathbf{r}, t)|^2}$  on the screen can be expressed in terms of the correlation function  $G(\mathbf{r}_2, t_2; \mathbf{r}_1, t_1)$

$$I(t) \propto G(1, 1) + G(2, 2) + 2\text{Re } G(2, 1), \quad (47)$$

$$G(\mathbf{r}_2, t_2; \mathbf{r}_1, t_1) = \langle \mathcal{E}^{(-)}(\mathbf{r}_2, t_2) \mathcal{E}^{(+)}(\mathbf{r}_1, t_1) \rangle. \quad (48)$$

$G(2, 1)$  is short for  $G(\mathbf{r}_2, t_2; \mathbf{r}_1, t_1)$  etc., and  $\mathcal{E}^{(\pm)}(\mathbf{r}, t) \propto \exp(\mp i\omega t)$  denote the positive/negative frequency components of the light wave. It is seen from Eq. (47) that the intensity on the second screen consists of three contributions: The first two terms represent the intensities caused by each of the pinholes in the absence of the other, whereas the third term gives rise to interference effects. [Note the difference between  $G(2, 1)$  and (45)].

For a superposition of many (uncorrelated) modes we obtain

$$\mathcal{E}(\mathbf{r}, t) = \sum_{\mathbf{k}} A_{\mathbf{k}} e^{i(\mathbf{k}\mathbf{r} - \omega_{\mathbf{k}}t)} + cc = \mathcal{E}^{(+)}(\mathbf{r}, t) + \mathcal{E}^{(-)}(\mathbf{r}, t), \quad (49)$$

$$G(2, 1) = \sum_{\mathbf{k}} |A_{\mathbf{k}}|^2 e^{i[\mathbf{k}(\mathbf{r}_2 - \mathbf{r}_1) - \omega_{\mathbf{k}}(t_2 - t_1)]}. \quad (50)$$

<sup>6</sup> The Michelson interferometer and the stellar interferometer would be even better suited instruments to measure the spatial and temporal coherence independently[18].

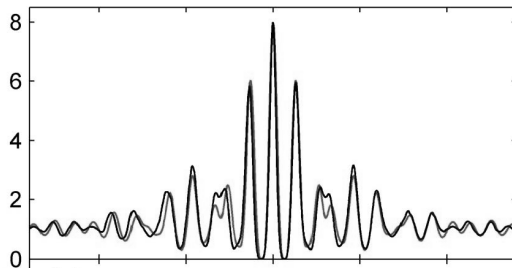


Figure 10. Experimental autocorrelation function of a 5fs laser oscillator at 82MHz and its spectral reconstruction (“background” = 1, time: in units of 10 fs). From Wegener[19].

In particular, for a gaussian spectral line centered at  $\omega_0$  (and  $\mathbf{r}_2 = \mathbf{r}_1$ ), Eq. (50) becomes

$$I(\omega) = \exp \left[ -\frac{(\omega - \omega_0)^2}{2(\Delta\omega)^2} \right], \quad (51)$$

$$G(t_2, t_1) = \int_{-\infty}^{\infty} I(\omega) e^{-i\omega(t_2 - t_1)} \frac{d\omega}{2\pi}, \quad (52)$$

$$= e^{-i\omega_0(t_2 - t_1)} \exp \left[ -\frac{1}{2} [\Delta\omega(t_2 - t_1)]^2 \right]. \quad (53)$$

Eq.(52) gives an example of the famous Wiener-Khinchine theorem[13]: the correlation function is just the Fourier-transformed power spectrum  $I(\omega_{\mathbf{k}}) \propto |A_{\mathbf{k}}|^2$ . Filtering in frequency-space is intimately related to a correlation (or coherence)–time  $\Delta t \propto 1/\Delta\omega$ , see Figs. 8 and 9. [Similarly, spatial filtering, i.e., selecting  $\mathbf{k}$ –directions within  $\Delta\mathbf{k}$  leads to spatial coherence.]

There is a deep relation between the fluctuations in thermal equilibrium (i.e. loss of coherence) and dissipation in a nonequilibrium state driven by an external force. This is the *fluctuation – dissipation theorem* which (for the example of Ch.3) reads

$$\eta = \frac{1}{2k_{\text{B}}T} K_{\text{FF}}(\omega = 0). \quad (54)$$

Analogous to optics, coherence can be defined for any quantity which is additive and displays a phase or has a vector character, e.g., electrical and acoustic “signals”, electromagnetic fields, wave–functions, etc. Coherence is intimately connected with reversibility, yet the opposite is not always true. At first sight, a process might appear as fully incoherent or random, nevertheless it may represent a highly correlated pure state which always implies complete coherence.

A beautiful example of an disguised coherent process is the spin– (or photon–) echo[20]. This phenomenon is related to a superposition of many

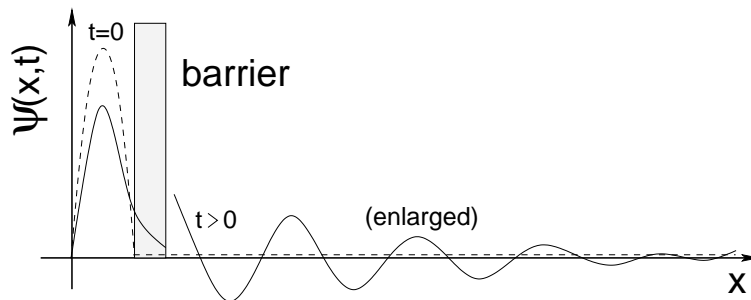


Figure 11. Gamow-decay of a metastable state by tunneling through a barrier.

sinusoidal field components with fixed (but random) frequencies. At  $t = 0$  these components have zero phase differences and combine constructively to a nonzero total amplitude. Later, however, they develop large random phase differences and add up more or less to zero so that the signal resembles “noise”. Nevertheless, there are fixed phase relations between the components at every time. By certain manipulations at time  $T$  a time-reversal operation can be realized which induces an echo at time  $t = 2T$ , which uncovers the hidden coherent nature of the state. Echo phenomena are always strong indications of hidden reversibility and coherence. For applications in semiconductor optics (photon-echo) see, Klingshirn[21], Haug and Koch[22], or previous Erice contributions[1](b). Another nice example is “weak localization” of conduction electrons in disordered materials[23].

A survey of second order coherence and the Hanbury-Brown Twiss effect can be found in Ref.[1](d).

## 5. Relaxation and Decoherence in Quantum Systems

### 5.1. DECAY OF A METASTABLE STATE

The exponential form of the radioactive decay  $N(t) = N_0 \exp(-\lambda t)$  (or time dependence of the spontaneous emission from an excited atom) follows from a simple assumption which can be hardly weakened:  $\dot{N} = -\lambda N$ . Nevertheless, numerous authors have pointed out that the exponential decay law is only an approximation and deviations from purely exponential behaviour are, in fact, expected at very short and very long times, e.g., Refs.[24].

At short times the decay of any nonstationary state must be quadratic

$$|\Psi(t)\rangle = e^{-it\hat{H}/\hbar} |\Psi(0)\rangle = \left[ 1 + (-it\hat{H}/\hbar) + \frac{1}{2}(\dots)^2 + \dots \right] |\Psi(0)\rangle, \quad (55)$$

$$N(t) = |\langle \Psi(0) | \Psi(t) \rangle|^2 = 1 - (\Delta\hat{H}/\hbar)^2 t^2 + \dots \quad (56)$$

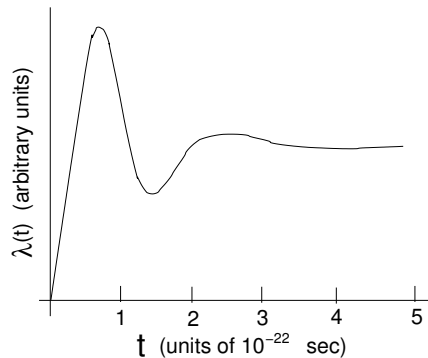


Figure 12. Calculated decay rate as a function of time. According to Avignone[26].

Here,  $N(t)$  denotes the non-decay probability and  $\Delta\hat{H}$  is the energy-uncertainty in the initial state. Clearly, the transition rate  $\lambda = -\dot{N} \propto t \rightarrow 0$  decreases linearly with  $t \rightarrow 0$ .<sup>7</sup>

On the other hand, at very long times the decay follows a power law  $N \propto t^{-\alpha}$  which originates from branch cuts in the resolvent operator[24](a,b). Nevertheless, pure exponential decay can arise if the potential  $V(x)$  decreases linearly at large distances, see, e.g., Ludviksson[24](c).

Up to date all experimental attempts to find these deviations failed[25]. For example, Norman et al.[25](d) have studied the  $\beta$ -decay of  $^{60}\text{Co}$  at times  $\leq 10^{-4}T_{1/2}$  ( $T_{1/2} = 10.5\text{min}$ ) and those of  $^{56}\text{Mn}$  over the interval  $0.3T_{1/2} \leq t \leq 45T_{1/2}$  ( $T_{1/2} = 2.579\text{h}$ ) to search for deviations from exponential decay but with a null result. Calculations by Avignone[26]

$$\lambda(t) = \frac{t}{\hbar^2} \int |\langle \Psi_f | \hat{H}_{\text{int}} | \Psi_i \rangle|^2 \left[ \frac{\sin(\frac{1}{2}\omega t)}{(\frac{1}{2}\omega t)} \right]^2 \rho(E_f) dE_f, \quad (57)$$

demonstrate, however, that these experiments were 18 – 20 orders of magnitude less time sensitive than required to detect pre-exponential decay, see Fig. 12.  $\hbar\omega = [E_\gamma - (E_i - E_f)]$ ,  $E_{i,f}$  are the nuclear eigenstate energies,  $\Psi_{i,f}$  are the initial and final states of the total system “nucleus + radiation”, and  $\rho(E_f)$  is the density of final states. For long times [...]  $\rightarrow 2\pi\delta(\omega)/t$  yielding Fermi’s Golden rule and a constant value of  $\lambda$  for  $t > 10^{-22}\text{s}$ .

Another example is the decay of an excited atom in state  $a$  which decays into the ground state  $b$  by spontaneous emission of a photon. The state of combined system “atom + radiation field” is

$$|\Psi(t)\rangle = c_a(t)|a, 0_{\mathbf{k}}\rangle + \sum_{\mathbf{k}} c_{b,\mathbf{k}}(t)|b, 1_{\mathbf{k}}\rangle. \quad (58)$$

<sup>7</sup> This may also have far reaching consequences for the interpretation of the predicted proton-decay[25](c) ( $T_{1/2} \approx 10^{15}$  times the age of the universe).

From the Schrödinger equation we get two differential equations for  $c_a, c_b$  which can be solved in the *Weisskopf–Wigner approximation*[27, 29](Ch. 6.3) which leads to pure exponential decay,

$$\dot{c}_a(t) = -\frac{\Gamma}{2}c_a(t), \quad |c_a(t)|^2 = \exp(-\Gamma t), \quad \Gamma = \frac{1}{4\pi\epsilon_0} \frac{4\omega_0^3 \mathbf{p}_{ab}^2}{3\hbar c^3}. \quad (59)$$

$\mathbf{p}_{ab}$  is the dipol–matricelement and  $\omega_0 = (E_a - E_b)/\hbar$ .

In an infinite system (as assumed above) the decay of a metastable state into another (pure) state is irreversible, yet it is not related to dissipation or decoherence – the dynamics is fully described by the (reversible) Schrödinger equation. Here, irreversibility stems from the boundary condition at infinity (“Sommerfeld’s Ausstrahlungsbedingung”). Although there is little chance to reveal the quadratic onset in spontaneous decay of an atom in vacuum it may show up in a photonic crystal[30]. For induced transitions it became, indeed, already feasible, where it is called quantum–Zeno (or “watchdog”) effect, see, e.g., Refs[31]. The decay of a metastable state has also received much attention for macroscopic tunneling processes[32].

## 5.2. DISSIPATIVE QUANTUM MECHANICS

On a microscopic level, dissipation, relaxation and decoherence are caused by the interaction of a system with its *environment* – dissipative systems are *open systems*. In contrast to classical (Newtonian) mechanics, however, in quantum systems dissipation cannot be included phenomenologically just by adding “friction terms” to the Schrödinger equation because

(a) dissipative forces cannot be included in the Hamiltonian of the system,  
 (b) irreversible processes transform a pure state to a mixed state which is described by a statistical operator  $\hat{\rho}$  rather than a wave function. Some useful properties are:

- $\hat{\rho}$  is a hermitian, non–negative operator with  $\text{tr}\hat{\rho} = 1$ .
- For a pure state  $\hat{\rho} = |\Psi\rangle\langle\Psi|$  is a projector onto  $|\Psi\rangle$ .
- General mixed state:  $\hat{\rho} = \sum_{\alpha} p_{\alpha} |\phi_{\alpha}\rangle\langle\phi_{\alpha}|$  with  $0 \leq p_{\alpha} \leq 1$ ,  $\sum_{\alpha} p_{\alpha} = 1$ .
- The dynamics of the total system is governed by the (reversible) *v. Neumann equation*

$$\frac{\partial}{\partial t}\hat{\rho}(t) + \frac{i}{\hbar}[\hat{H}, \hat{\rho}] = 0. \quad (60)$$

- To construct the density operator of the “reduced system”  $\hat{\rho}_s = \text{tr}_{\text{res}}\hat{\rho}$  one has to “trace–out” the reservoir variables which leads to irreversible behaviour governed by the *master equation*

$$\frac{\partial}{\partial t}\hat{\rho}_s(t) + \frac{i}{\hbar}[\hat{H}_s, \hat{\rho}_s] = \hat{C}(\hat{\rho}_s), \quad (61)$$

where  $\hat{C}(\hat{\rho}_s)$  is the collision operator.

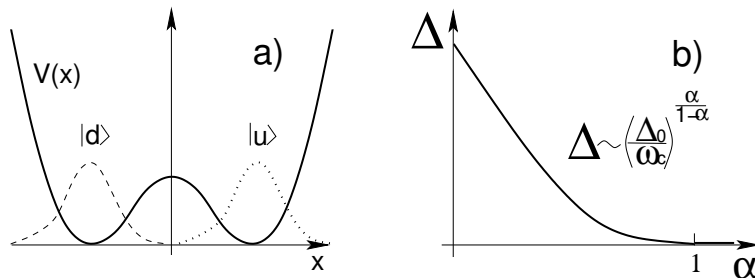


Figure 13. (a) Double well potential with localized base states  $|d\rangle$  (“down”),  $|u\rangle$  (“up”). (b) Renormalized level splitting as a function of damping.

A simple approximation for  $\widehat{C}(\widehat{\rho}_r)$  is the *relaxation–time–approximation*

$$\widehat{C}(\widehat{\rho}_s) = -\frac{1}{\tau}(\widehat{\rho}_s(t) - \widehat{\rho}_s^{\text{eq}}), \quad (62)$$

where  $\widehat{\rho}_s^{\text{eq}}$  denotes the statistical operator for the equilibrium state. In general, relaxation times  $\tau$  for the diagonal and non–diagonal elements of  $\widehat{\rho}_s$  are different, the relaxation goes to a local equilibrium with a  $(\mathbf{r}, t)$ –dependent temperature and chemical potential[33], and memory effects may occur.

Finally we mention the *fluctuation–dissipation theorem* which establishes an important relation between the fluctuations in equilibrium of two observables  $\widehat{A}, \widehat{B}$  and the dissipative part of the linear response of  $\widehat{A}$  upon a perturbation  $\widehat{H}_{\text{int}} = -\widehat{B}b(t)$ [13]. Nowadays dissipative quantum mechanics has become an important issue in the field of mesoscopic systems[16, 28] and quantum optics[29], see also contributions at previous Erice schools[1](a,c).

### 5.3. TWO LEVEL SYSTEMS (TLS)

We study a system with two base states  $|u\rangle, |d\rangle$  with equal energies  $\epsilon_0$ , e.g., a particle in a double–well potential, see Fig. 13.

$$|u\rangle = \begin{pmatrix} 1 \\ 0 \end{pmatrix}, \quad |d\rangle = \begin{pmatrix} 0 \\ 1 \end{pmatrix}, \quad (63)$$

In this base, the Hamiltonian and the (electrical) dipole operator read

$$\widehat{H}_0 = \begin{pmatrix} \epsilon_0 & -\Delta \\ -\Delta & \epsilon_0 \end{pmatrix}, \quad \widehat{D} = d_0 \begin{pmatrix} 1 & 0 \\ 0 & 1 \end{pmatrix}. \quad (64)$$

Here,  $\pm\Delta$  is the tunneling splitting and  $d_0 = ex_0$  is the magnitude of the (electrical) dipole moment. The eigenstates of  $\widehat{H}_0$  are

$$|1\rangle = \frac{1}{\sqrt{2}} \begin{pmatrix} 1 \\ 1 \end{pmatrix}, \quad |2\rangle = \frac{1}{\sqrt{2}} \begin{pmatrix} 1 \\ -1 \end{pmatrix}. \quad (65)$$

In the basis of these energy–eigenstates  $|1, 2\rangle$ , we have ( $\epsilon_{1,2} = \epsilon_0 \mp \Delta$ )

$$\hat{H}_0 = \begin{pmatrix} \epsilon_1 & 0 \\ 0 & \epsilon_2 \end{pmatrix}, \quad \hat{D} = d_0 \begin{pmatrix} 0 & 1 \\ 1 & 0 \end{pmatrix}. \quad (66)$$

For the TLS, the density operator is a  $2 \times 2$  matrix  $\hat{\rho} = \rho_{i,k}$ . In particular, for a pure state  $|\Psi\rangle = c_1|1\rangle + c_2|2\rangle$ , we have

$$\hat{\rho}_{\text{pure}} = |\psi\rangle\langle\psi| = \begin{pmatrix} |c_1|^2 & c_1 c_2^* \\ c_1^* c_2 & |c_2|^2 \end{pmatrix}. \quad (67)$$

The diagonal elements  $\rho_{11}$  and  $\rho_{22}$  yield the populations, whereas the off–diagonal elements describe the coherent motion of the dipole moment  $d = \text{tr}(\hat{\rho}\hat{D}) \propto \text{Re}\rho_{12}$ .

We consider a TLS subjected to a time–dependent electrical field  $\mathcal{E}(t)$

$$\hat{H} = \hat{H}_0 - \mathcal{E}(t)\hat{D}. \quad (68)$$

The v. Neumann–master equation (61) (in the basis of  $\hat{H}_0$  eigenstates) reads

$$\dot{\rho}_{11}(t) + 2\omega_{\text{R}}(t)\text{Im}(\rho_{21}) = -\frac{1}{T_1}(\rho_{11} - \rho_{11}^{\text{eq}}), \quad (69)$$

$$\dot{\rho}_{22}(t) - 2\omega_{\text{R}}(t)\text{Im}(\rho_{21}) = -\frac{1}{T_1}(\rho_{22} - \rho_{22}^{\text{eq}}), \quad (70)$$

$$\left[\frac{d}{dt} + i\omega_0\right]\rho_{21}(t) - i\omega_{\text{R}}(t)(\rho_{22} - \rho_{11}) = -\frac{1}{T_2}\rho_{21}. \quad (71)$$

$\omega_0 = (\epsilon_2 - \epsilon_1)/\hbar = 2\Delta/\hbar$  is the transition frequency,  $\omega_{\text{R}}(t) = p_0\mathcal{E}(t)/\hbar$  denotes the (time dependent) Rabi–frequency and  $\hat{\rho}^{\text{eq}} = \exp(-\hat{H}_0/k_{\text{B}}T)/Z$ .  $Z$  is the partition function. The diagonal elements  $\rho_{11}$ ,  $\rho_{22}$  give the population of the stationary states  $|1\rangle, |2\rangle$ , whereas the population of the “up” and “down” states and the dipole moment are determined by  $\rho_{12} = \rho_{21}^*$

$$N_{\text{u}}(t) = \text{tr}(\hat{\rho}(t)|u\rangle\langle u|) = \frac{1}{2} + \text{Re}\rho_{12}(t), \quad (72)$$

$$d(t) = \text{tr}(\hat{\rho}(t)\hat{D}) = 2d_0\text{Re}\rho_{12}(t). \quad (73)$$

Usually, Eqs. (69–71) are rewritten in terms of the inversion  $I = \rho_{22} - \rho_{11}$  and (complex) dipole moment  $\mathcal{P} = \rho_{21}$  or in terms of a pseudo spin vector  $\mathbf{s}(t) = \text{tr}(\hat{\rho}\hat{\boldsymbol{\sigma}})$ , where  $\hat{\boldsymbol{\sigma}}$  is the Pauli–spin–vector operator.

$$\frac{d\mathbf{s}(t)}{dt} = \boldsymbol{\Omega} \times \mathbf{s} + C(\mathbf{s}), \quad \boldsymbol{\Omega} = (-2\omega_{\text{R}}(t), 0, -\omega_0). \quad (74)$$

The *Bloch equations* (74) permit a very suggestive physical interpretation: they describe the rotation of vector  $\mathbf{s}$  around  $\boldsymbol{\Omega}$ . For applications in atomic

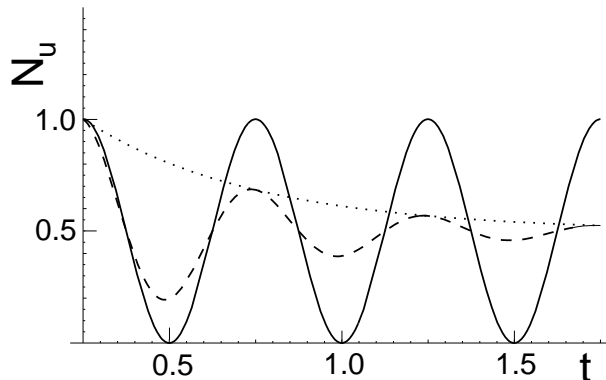


Figure 14. Dynamics of the population of the “up” state of the two-level-system  $N_u(t)$ : Coherent (solid line), relaxing (dashed line), and fully incoherent motion (dotted line).

physics see, e.g., books by Allen and Eberly[20], semiconductor optics see Klingshirn[21], Haug and Koch[22], and previous Erice contributions[1](c).

As an illustration we discuss the following situations:

(a) At  $t = 0$  the system is in the excited stationary state  $|2\rangle$

$$\rho_{11}(t) = \rho_{11}^{\text{eq}}(1 - e^{-t/T_1}), \quad \rho_{21}(t) = 0. \quad (75)$$

(b) At  $t = 0$  the system is in the “up” state

$$\rho_{11}(t) = \frac{1}{2}e^{-t/T_1} + \rho_{11}^{\text{eq}}(1 - e^{-t/T_1}), \quad \rho_{21}(t) = \frac{1}{2}e^{-i\omega_0 t}e^{-t/T_2}. \quad (76)$$

(c) For larger damping, one may neglect the coherent motion between states  $|u\rangle$ ,  $|d\rangle$  and set up rate equations for the diagonal elements  $\dot{N}_m = \rho_{mm}$

$$\dot{N}_m(t) = \sum_n (N_n \Gamma_{n \rightarrow m} - N_m \Gamma_{m \rightarrow n}), \quad (77)$$

$$\Gamma_{n \rightarrow m} \exp(-E_n/k_B T) = \Gamma_{m \rightarrow n} \exp(-E_m/k_B T). \quad (78)$$

Eq. (78) is the *detailed balance* relation.

In our case  $|u\rangle$ ,  $|d\rangle$  have the same energy so that  $\Gamma_{u \rightarrow d} = \Gamma_{d \rightarrow u} = \Gamma$ . Using  $N_u + N_d = 1$ , Eqs. (77) can be solved easily, e.g., for  $N_u(0) = 1$ ,  $N_d(0) = 0$ , we obtain

$$N_u(t) = \frac{1}{2}(1 + e^{-2\Gamma t}), \quad N_d(t) = \frac{1}{2}(1 - e^{-2\Gamma t}). \quad (79)$$

Some results of coherent, fully incoherent, and relaxation dynamics are displayed in Fig.14.

The “state of the art” treatment of the dissipative TLS is laid out in the review article by Leggett et al.[34] and the book by Weiss[35]. The

underlying model is

$$\hat{H} = \frac{1}{2}\hbar\Delta\hat{\sigma}_x + \frac{1}{2}q_0\hat{\sigma}_z \sum_i c_i x_i + \hat{H}_{\text{res}}, \quad (80)$$

$$\alpha = \eta q_0^2 / 2\pi\hbar, \quad J(\omega) = \eta\omega e^{-\omega/\omega_c}. \quad (81)$$

$\omega_c$  denotes a cut-off in the excitation spectrum. For finite temperatures and small coupling to the bath  $0 < \alpha < 1$  the levels become damped as well as the splitting  $\omega_0$  becomes smaller and eventually tends to zero at  $\alpha = 1$ , see Fig. 13(b). This conforms with the classical harmonic oscillator. [The path integral techniques as well as the explicit results are too involved to be discussed here.]

When the oscillation frequency  $\omega_0$  of the TLS is small compared with the Debye-frequency, there is a universal lower bound on the decoherence rate  $\Gamma \ll \omega_0$  due to the atomic environment[36]

$$\langle x(t)x(0) \rangle = x_0^2 e^{-\Gamma t} \cos(\omega_0 t), \quad \Gamma = \frac{M^2 x_0^2 \omega_0^5}{2\pi\hbar\rho c_s^3} \coth\left(\frac{\hbar\omega_0}{2k_B T}\right). \quad (82)$$

$\rho$  denotes the mass density, and  $c_s$  the speed of sound. For a  $NH_3$  molecule ( $M = 3 \times 10^{-23}$  g,  $\omega_0 = 10^{12}$ /s,  $x_0 = 2 \times 10^{-8}$  cm,  $\rho = 5$  g/cm<sup>3</sup>,  $c_s = 10^5$  cm/s)  $\Gamma \approx 10^{10}$ /s. For tunneling electrons the rate is much smaller.

Kinetic equations in the Markovian limit are derived in Refs.[44, 45].

### 5.3.1. The neutral Kaon system

Particle physics has become an interesting testing ground for fundamental questions in quantum physics, e.g. possible deviations from the quantum mechanical time evaluation have been studied in the neutral Kaon system[39]. These particles are produced by strong interactions in strangeness eigenstates ( $S = \pm 1$ ) and are termed  $K_0$   $\bar{K}_0$  which are their respective antiparticles. As both particles decay (by weak forces) along the same channels (predominantly  $\pi^\pm$  or two neutral pions) there is an amplitude which couples these states. The ‘‘stationary’’ (CP-eigenstates) called  $K_s$  and  $K_l$  for ‘‘short’’ and ‘‘long’’ (or  $K_1, K_2$ ). Decay of  $K_s$  and  $K_l$  (by weak forces), however, is very different and results from CP-violation.  $K_s$  decays predominantly into 2 pions with  $\tau_s = 9 \times 10^{-10}$ s whereas, the  $K_l$  decay is (to lowest order) into 3 pions with  $\tau_l = 5 \times 10^{-8}$ s, [39]. The oscillatory contribution in the decay rate corresponds to a small  $K_s/K_l$  level splitting of  $\Delta m_{K_0}/m_{K_0} \approx 4 \times 10^{-18}$ . For an overview see, *The Feynman Lectures on Physics*[37] (Vol. III, Ch. 11-5) and Källén’s textbook[38].

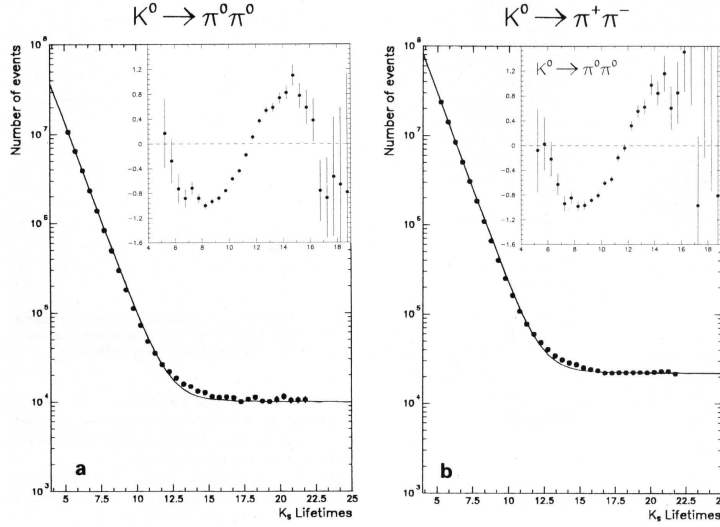


Figure 15. The rate of decay of Kaons to neutral and charged pions as a function of  $K_s$  life-time. Superimposed are the fitted lifetime distributions with the interference terms removed. The insets (interchanged?) show the interference terms extracted from the data. From Carosi et al.[39](a).

#### 5.4. A PARTICLE IN A POTENTIAL

For the harmonic oscillator interacting with a reservoir Caldeira and Leggett [15] and Walls[40] provided an exact solution which shows a rich and intricate dependence on the parameters – too extensive to be discussed here. For weak coupling and high temperatures, however, the physics can be described by an equation of motion for the reduced density operator  $\rho(x, x', t) = \langle x | \hat{\rho}_s | x' \rangle$  of the following form[41] (p. 57)

$$\begin{aligned} \frac{\partial}{\partial t} \rho(x, x'; t) + \frac{i}{\hbar} (\hat{H} - \hat{H}') \rho(x, x'; t) = \\ = -\frac{\gamma}{2} (x - x') \left( \frac{\partial}{\partial x} - \frac{\partial}{\partial x'} \right) \rho(x, x'; t) \\ - \Lambda (x - x')^2 \rho(x, x'; t), \end{aligned} \quad (83)$$

$$\hat{H} = -\frac{\hbar^2}{2m} \frac{\partial^2}{\partial x^2} + V(x). \quad (84)$$

$\hat{H}'$  is given by (84) by replacing  $x$  by  $x'$ . Eq. (83) is valid for a particle in an arbitrary potential. Relaxation rate  $\gamma$  and decoherence parameter  $\Lambda$  are considered as independent parameters. Scattering of the oscillator particle by a flux of particles from the environment enforces decoherence with a rate of

$$\Lambda = nv\sigma_{sc}k^2. \quad (85)$$

TABLE I. Some values of the localization rate (1/s). From Joos in Ref.[41].

	free electron	$10^{-3}$ cm dust particle	bowling ball
sunlight on earth	10	$10^{20}$	$10^{28}$
300K photons	1	$10^{19}$	$10^{27}$
3K cosmic radiation	$10^{-10}$	$10^6$	$10^{17}$
solar neutrinos	$10^{-15}$	10	$10^{13}$

$nv$  is the flux and  $k$  the wave number of the incoming particles with cross section  $\sigma_{sc}$ . For a recent paper on collisional decoherence see Ref.[43].

#### 5.4.1. Free particles

First, we consider a superposition of two plane waves without coupling to the bath

$$\Psi(x, t = 0) = \frac{1}{2} \left( e^{ik_1x} + e^{ik_2x} \right), \quad (86)$$

$$\rho_0(x, x'; t) = \Psi(x, t)\Psi^*(x', t), \quad (87)$$

$$\rho_0(x, x; t) = 1 + \cos \left[ (k_1 - k_2)x + \frac{\hbar(k_1^2 - k_2^2)}{2m}t \right]. \quad (88)$$

In the presence of the environment, the fringe contrast in the mean density will be reduced[40] (For notational simplicity, explicit results are for the particle density, i.e. the diagonal elements of  $\hat{\rho}$  only.)

$$\rho(x, x; t) = 1 + e^{-\eta} \cos \left[ (k_1 - k_2)x - \frac{1 - e^{-\gamma t}}{\gamma} \frac{\hbar(k_1^2 - k_2^2)}{2m}t \right], \quad (89)$$

$$\eta = \frac{2\hbar^2\Lambda}{m^2\gamma^3} \left[ \gamma t/2 - \frac{3}{4} + e^{-\gamma t} - \frac{1}{4}e^{-2\gamma t} \right] (k_1^2 - k_2^2). \quad (90)$$

In the special case of negligible friction,  $\gamma = 0$ , the visibility of the interference fringes is strongly reduced, while the spatial structure remains unaffected.

The standard example of a gaussian wave packet with momentum  $\hbar k_0$  and width  $a$  can also be tackled analytically, but the result is rather lengthy, hence we only state the result for the mean position and variance

$$\langle x \rangle = \frac{\hbar k_0}{m\gamma} (1 - e^{-\gamma t}), \quad (\Delta x)^2 = \frac{a^2}{2} \left( 1 + \left[ \frac{\hbar t}{ma^2} \right]^2 \right) + \frac{\hbar^2\Lambda}{m^2} t^3. \quad (91)$$

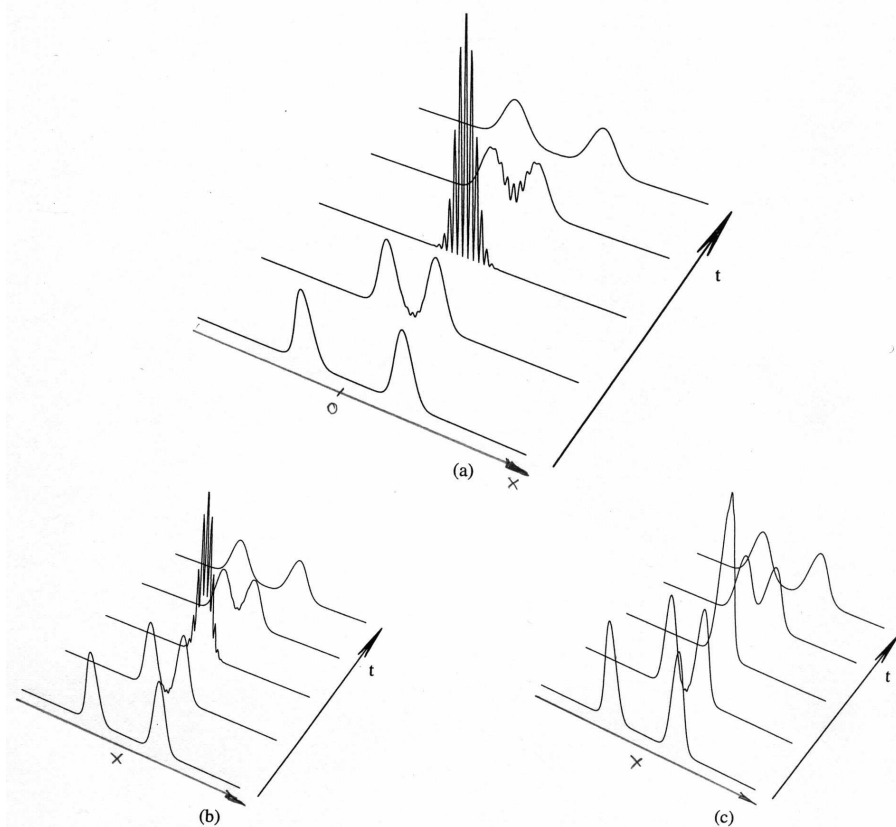


*Figure 16.* Harmonic oscillator which is initially in a superposition of two displaced ground state wave functions at  $x = \pm x_0$ . (a) pure quantum mechanics, (b) weak damping, (c) strong damping. Loss of coherence is much stronger than the damping of the oscillation amplitude. According to Joos' article in Ref.[41] (p. 35–135).

Note,  $\langle x \rangle$  is independent of  $\Lambda$  whereas  $\Delta x$  is independent of  $\gamma$ . For details, see appendix A2 of Giulini's book[41].

#### 5.4.2. Harmonic oscillator

When the two components of a wave function (or mixed state) do not overlap, a superposition of two spatially distinct wave packets can still be distinguished from a mixture, when the two wave packets are brought to interference as in the two-slit experiment. In general, the decoherence time is much smaller than the relaxation time  $1/\gamma$

$$\tau_{\text{dec}} = \frac{1}{\gamma} \left( \frac{\lambda_{\text{dB}}}{\Delta x} \right)^2. \quad (92)$$

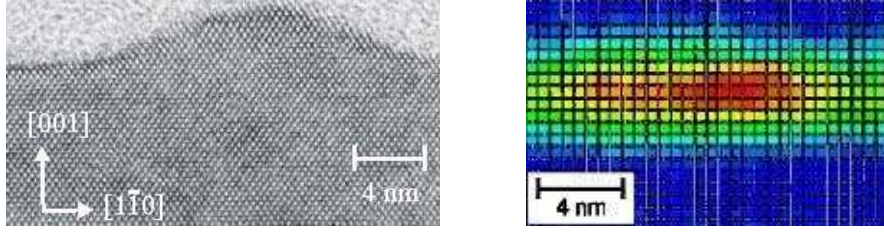


Figure 17. High resolution transmission electron micrographs of InAs/GaAs QDs (vertical and horizontal cross sections)[46].

$\lambda_{dB} = \hbar/\sqrt{2mk_B T}$  is the thermal de Broglie wave length and  $\Delta x$  is the width of the wave packet. For macroscopic parameters  $m = 1g$ ,  $\Delta x = 1cm$  the decoherence time  $\tau_{dec}$  is smaller than the relaxation time  $\gamma$  by an enormous factor of  $\sim 10^{40}$ . This is the every day experience of the absence of interference phenomena in the macroscopic world. For the harmonic oscillator, this is easily seen from a superposition of two counterpropagating gaussian packets, see Fig. 16. A spectacular example is the interference of two Bose–Einstein condensates, see Wieman’s Erice–article in Ref.[1](e).

## 6. Exciton Spins in Quantum Dots

The current interest in the manipulation of spin states in semiconductor nanostructures originates from the possible applications in quantum information processing[2]. Since most of the present concepts for the creation, storage and read–out of these states are based on (or involve) optical techniques one has to investigate the dynamics and relaxation of exciton (or trion) states rather than single carrier–spin states. Due to the discrete energy structure of quantum dots (QDs), inelastic relaxation processes are strongly suppressed with respect to quantum wells or bulk systems, e.g.,  $\tau_{bulk} \approx 10ps$  whereas  $\tau_{QD} \approx 20ns$ .

Extensive experimental studies have identified the main features of the exciton fine structure in self–organized QDs by single–dot spectroscopy. Such QDs are usually strained and have an asymmetrical shape with a height smaller than the base size, see Fig. 17. The reduction of the QD symmetry lifts degeneracies among the exciton states and results, in particular, in a splitting of the exciton ground state. Thus, as a consequence of strain and confinement, the ground states of the QD heavy–hole (hh) and light–hole (lh) excitons are well-separated [ $E_{h-1} \approx 30 \dots 60meV$ ] and the hh–exciton has the lowest energy, see Fig. 18(a-c). For an overview on optical properties of semiconductor quantum structures see Refs.[47](a,b).

The hh– and lh–exciton quartets are characterized by the projections  $J_z = \pm 1, \pm 2$  and  $J_z = \pm 1, 0$  of the total angular momenta  $J = 1, 2$ , res-

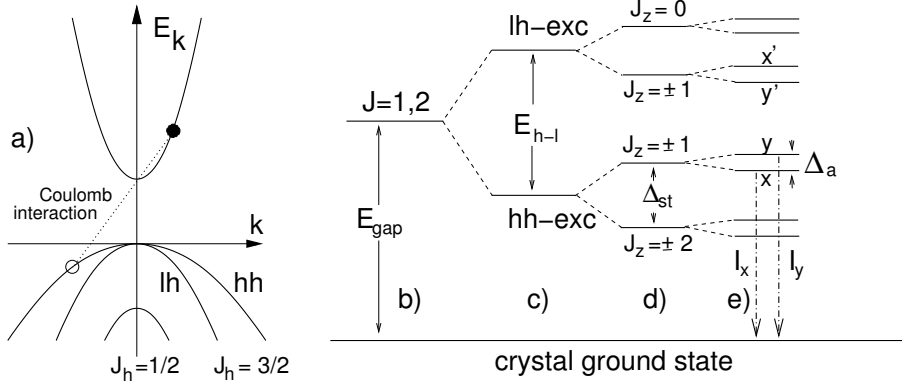


Figure 18. Sketch of bandstructure and exciton levels in III-V quantum dots ( $J_h = 1/2$  split-off band and bulk heavy-light hole exciton splitting omitted).

pectively. The short-range exchange interaction splits the ground states of both hh- and lh-excitons into doubles [so-called singlet-triplet splitting,  $\Delta_{st} \approx 0.2\text{meV}$ , in CdSe:  $1\text{meV}$ ], see Fig. 18(d). The lateral anisotropy of a QD leads to a further splitting of the  $|\pm 1\rangle$  levels (labeled by  $|x\rangle$  and  $|y\rangle$ ) with allowed dipole transitions to the crystal ground state which are linearly polarized along the two nonequivalent in-plane QD axes  $[1, \pm 1, 0]$ , see Fig. 18(e). This anisotropic splitting [ $\Delta_a \approx 0.1 \dots 0.2\text{meV}$ ] originates from the long-range exchange interaction in the elongated QDs.

Experimental studies on exciton-spin dynamics in QDs refer mostly to spin-coherence, i.e., they determine the transverse relaxation time  $T_2$ . Studies of the population relaxation of spin states (i.e. longitudinal relaxation time  $T_1$ ) are rare since they require strict resonant excitation conditions. The only direct experimental studies on population relaxation between  $|x\rangle$  and  $|y\rangle$  under perfect resonant excitation were done by Marie's group[49] (Toulouse, France). To improve the signal to noise ratio, an ensemble of nearly identical InAs-QDs in a microresonator was used, see Fig. 19. Experimentally, these depopulation processes are analyzed by detecting a decay of the polarization degree  $P = (I_x - I_y)/(I_x + I_y) = \exp(-t/\tau_{\text{pol}})$  of the luminescence upon excitation by a  $x$ - (or  $y$ -) polarized light pulse. ( $I_x, I_y$  denote the intensities of the  $x$ -,  $y$ -polarized luminescent radiation). The total intensity from both luminescent transitions to the crystal ground state is constant. Hence, relaxation is solely within the  $x$ - $y$  doublet. The incomplete polarization degree at time  $t = 0$  probably results from misalignment of the QDs in the microresonator. Despite the tiny  $x$ - $y$  splitting of about  $0.1 - 0.2\text{meV}$ , the relaxation is thermally activated with the LO-phonon energy of about  $30\text{meV}$ . In conclusion, exciton-spin is totally frozen during the radiative lifetime  $\tau_{\text{rad}} \approx 1\text{ns}$  (even for high magnetic fields up to  $8\text{T}$ ). With decreasing size, increasing temperature, and large magnetic fields,

however, the  $T_1$ -time becomes comparable to the exciton life-time. For details see Tsitsishvili[48](a,b).

Relaxation and decoherence on a single QD was studied by Henneberger's group[50] (Berlin, Germany) by analyzing time-resolved secondary emission. Because strict resonant excitation is faced with extreme stray light problems, LO-phonon assisted quasi-resonant excitation by tuning the laser source 28meV(=  $\hbar\omega_{LO}$ ) above the exciton ground state was used, see Fig. 20. The x/y doublet of the  $X_0$  exciton with its radiative coupling to the crystal ground state represents a "V-type" system[29], where quantum beats in the spontaneous emission may occur upon coherent excitation (spectral of the laser pulse larger than the level splitting). In the present case the doublet consists of two linearly cross-polarized components so that interference is possible only by projecting the polarization on a common axis before detection. For excitation into the continuum (of the wetting layer) the PL decay is monotonous with a single time constant  $1/\Gamma = 320\text{ps}$  which is the anticipated radiative life-time. The beat period (which by chance is also 320ps) corresponds to a fine structure splitting of  $13\mu\text{V}$ , not resolvable in the spectral domain. The fact that the beat amplitude decays with the same time-constant as the overall signal clearly demonstrates, no further relaxation and decoherence takes place once the exciton has reached the ground state doublet. However, a large 60% loss of the initial polarization degree of unknown origin was found.

## 7. Outlook

The transition between the microscopic and macroscopic worlds is a fundamental issue in quantum measurement theory[51]. In an ideal model of measurement, the coupling between a macroscopic apparatus ("meter") and a microscopic system ("atom") results in an entangled state of the "meter+atom" system. Besides the macroscopic variable of the display the meter supplies many uncontrolled variables which serve as a bath and irreversibly de-entangles the atom-meter state. For a recent overview on this field see contributions by Giulini[41] and Zurek[42, 52]. A nice overview on *Strange properties of Quantum Systems* has been given by Costa[1](d).

Brune et al.[53] created a mesoscopic superposition of radiation field states with classically distinct phases and, indeed, observed its progressive decoherence and subsequent transformation to a statistical mixture. The experiment involved Rydberg atoms interacting once at a time with a few photons coherent field in a high-Q cavity.

The interaction of the system with the environment leads to a discrete set of states, known as *pointer states* which remain robust, as their superposition with other states, and among themselves, is reduced by decoherence.

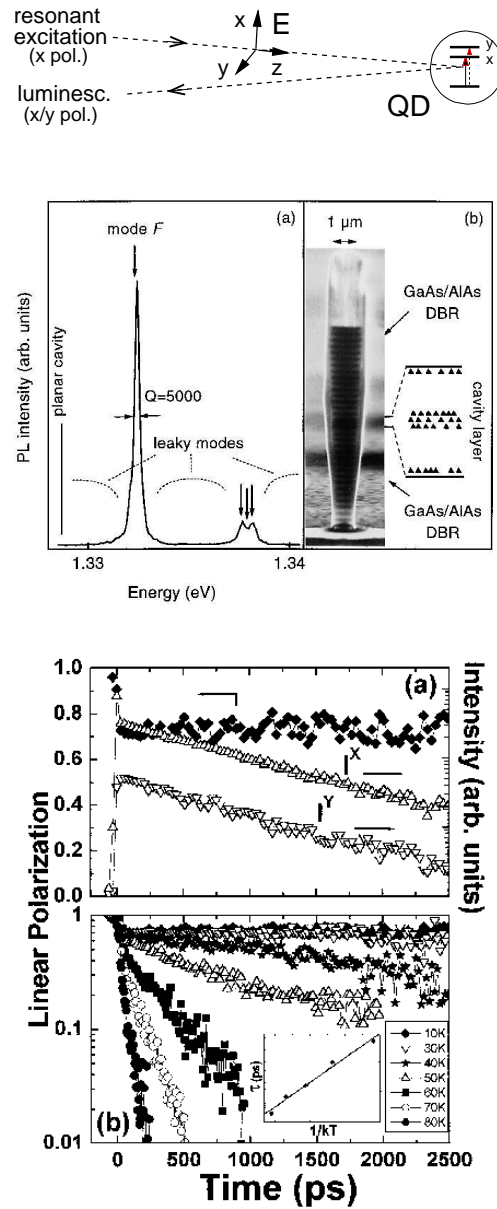
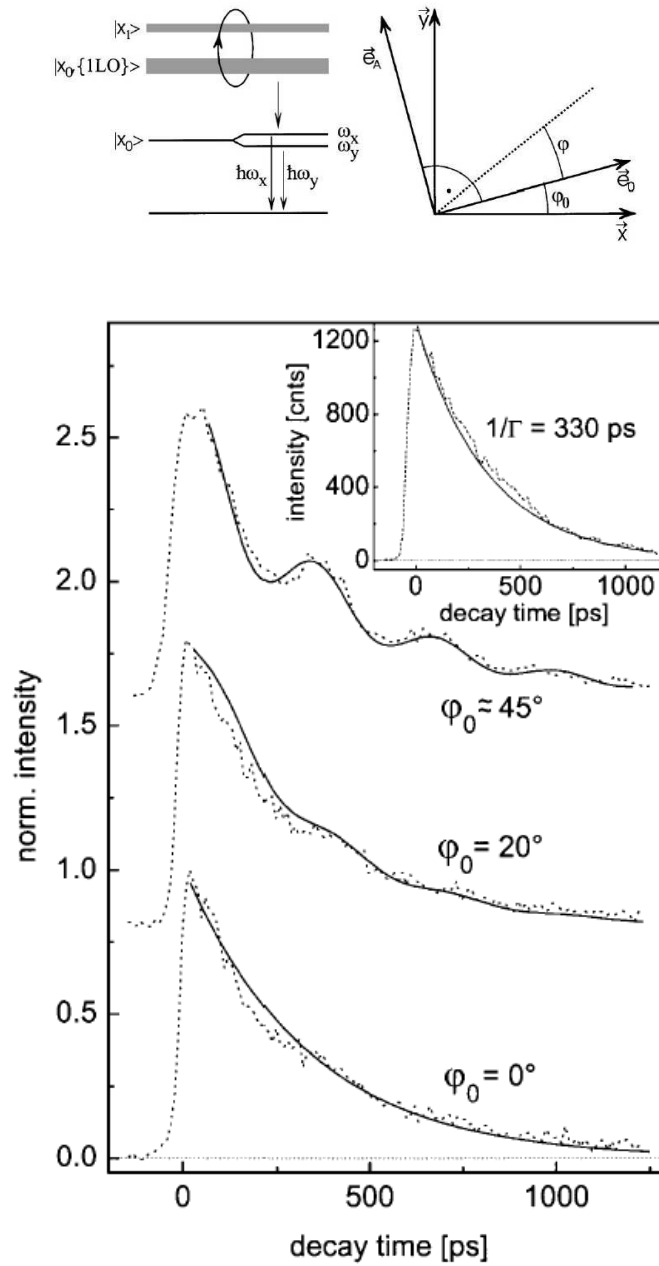


Figure 19. Experiment by Paillard et al.[49] on a system of many InAs/GaAs QDs. Upper panel: Setup, middle: microresonator structure, bottom: (a) Time dependence of the measured photoluminescence components copolarized  $I^x$  ( $\Delta$ ) and cross polarized  $I^y$  ( $\nabla$ ) to the  $\sigma^x$  polarized excitation laser ( $T = 10\text{K}$ ) and the corresponding linear polarization degree  $P_{\text{lin}}$  ( $\blacklozenge$ ). (b) Temperature dependence of the linear polarization dynamics. Inset:  $P_{\text{lin}}$  decay time as a function of  $1/(k_B T)$ .



*Figure 20.* Experiment by Flissikowski et al.[50] on a single CdSe/ZnSe QD. Upper panel: Energy level scheme (left) and geometry (right). Cross alignment of the polarizers for excitation ( $e_0$ ) and detection ( $e_A$ ). Lower panel: Relaxation and quantum beats in the photoluminescence for different angles with respect to the fundamental QD axis. Inset: Excitation into the continuum for comparison.

## 8. Acknowledgements

Thanks to Prof. Rino Di Bartolo and his team, the staff of the Majorana Center, and all the participants who again provided a wonderful time in a stimulating atmosphere. This work was supported by the DFG Center for Functional Nanostructures CFN within project A2.

## References

1. Proceedings of the International School of Atomic and Molecular Spectroscopy, Di Bartolo, B., et al. (Eds.), Majorana Center for Scientific Culture, Erice, Sicily:
  - (a) (1985) *Energy Transfer Processes in Cond. Matter*, NATO ASI B 114, Plenum;
  - (b) (1997) *Ultrafast Dynamics of Quantum Systems*, NATO ASI B 372, Plenum;
  - (c) (2001) *Advances in Energy Transfer Processes*, World Scientific;
  - (d) (2005) *Frontiers of Optical Spectroscopy*, Kluwer;
  - (e) (2006) *New Developments in Optics and Related Fields*, Kluwer (to appear).
2. (a) Bonadeo, N. H. et al. (1998), *Science*, **282**, 1473;
  - (b) Awschalom, D. D. et al. (Eds) (2002) *Semiconductor Spintronics and Quantum Computation*, Springer;
  - (c) Žutić, I. et al. (2004), *Rev. Mod. Phys.*, **76**, 323.
3. Haase, W. and Wröbel, S. (Eds.) (2003) *Relaxation Phenomena*, Springer.
4. Kohlrausch, R. (1854), *Poggendorffs Annalen der Physik und Chemie* **91**(1), 56.
5. Scher, H. et al. (1991), *Phys. Today*, Jan-issue, p. 26.
6. (a) Götze, W. and Sjögren, L. (1992), *Rep. Progr. Phys.* **55**, 241;
  - (b) Phillips, J. C. (1996), *Rep. Progr. Phys.* **59**, 1133;
  - (c) Jonscher, A. K. (1977), *Nature* **267**, 673.
7. Prudnikov, A. P. et al. (Eds) (1992) *Integrals and Series*, Gordon and Breach.
8. (a) Palmer, R. G. et al. (1984), *Phys. Rev. Lett.* **53**, 958;
  - (b) Sturman B. and Podilov, E. (2003), *Phys. Rev. Lett.* **91**, 176602.
9. Dressel, M. et al. (1996), *Phys. Rev. Lett.* **77**, 398.
10. Sokolov, I. M. et al. (Nov. 2002), *Physics Today*, p. 48.
11. (a) Liu, S. H. (1985), *Phys. Rev. Lett.* **55**, 529 and (1986), *PRL* **56**, 268;
  - (b) Kaplan, Th. et al. (1987), *Phys. Rev.* **B35**, 5379;
  - (c) Dissado, L. A. and Hill, R. M. (1987), *Phys. Rev.* **B37**, 3434.
12. (a) Zabel, I. H. H. and Strout, D. (1992), *Phys. Rev.* **B46**, 8132;
  - (b) Sidebottom, D. L. (1999), *Phys. Rev. Lett.* **83**, 983.
13. Reif, F. (1965) *Fundamentals of Statistical and Thermal Physics*, McGraw-Hill.
14. Einstein, A. (1905), *Annalen der Physik (Leipzig)*, **17**, 549.
15. Caldeira, A. O. and Leggett, A. J. (1985), *Phys. Rev. A* **31**, 1059.
16. Dittrich, T. et al. (Eds) (1998) *Quantum Transport and Dissipation*, Wiley-VCH.
17. Fick, E. and Sauermann, G. (1990) *The Quantum Statistics of Dynamic Processes*, Solid State Sciences **86**, (Springer, ).
18. Born, M. and Wolf, E. (1964) *Principles of Optics*, Pergamon.
19. Wegener, M, private communication.
20. Allen, L. and Eberly, H. (1975) *Optical Resonance and Two-Level Atoms*, Wiley.
21. Klingshirn, C. F. (2004) *Semiconductor Optics*, 3<sup>rd</sup> edition, Springer.
22. Haug, H. and Koch, S. W. (2004) *Quantum Theory of the Optical and Electronic Properties of Semiconductors*, World Scientific, 4<sup>th</sup> edition.

23. Bergmann, G. (1984), Phys. Rep. **107**, 1.
24. (a) Höhler, G. (1958), Z. Phys **152**, 546;  
 (b) Peres, A. (1980), Ann. Phys. (NY), **129**, 33;  
 (c) Ludviksson, A. (1987), J. Phys. A: Math. Gen. **20**, 4733.
25. (a) Wessner, J. M. et al. (1972), Phys. Rev. Lett. **29**, 1126;  
 (b) Horwitz, L. P. and Katznelson, E. (1983), Phys. Rev. Lett. **50**, 1184;  
 (c) Grotz, G. and Klapdor, H. V. (1984), Phys. Rev. C **30**, 2098;  
 (d) Norman, E. B. et al. (1988), Phys. Rev. Lett **60**, 2246;  
 (e) Koshino, K. and Shimizu, A. (2004), Phys. Rev. Lett. **92**, 030401.
26. Avignone, F. T. (1988), Phys. Rev. Lett. **61**, 2624.
27. Weisskopf, V. und Wigner, E. (1930), Z. Phys. **63**, 54.
28. Novotny, T. et al. (2003), Phys. Rev. Lett. **90**, 256801.
29. Scully, M. O. and Zubairy, M. S. (1997) *Quantum Optics*, Cambridge.
30. Busch, K. et al. (2000), Phys. Rev. E **62**, 4251.
31. (a) Itano, W. M. et al. (1990), Phys. Rev. A **41**, 2295; (1991) *ibid* **43**, 5165, 5166;  
 (b) Kwiat, P. et al. (Nov. 1996), Scientific American, 52.
32. (a) Leggett, A. J. (1978), J. Physique C **6**, 1264;  
 (b) Schmid, A. (1986), Ann. Phys. (N.Y.), **170**, 333.
33. Etzkorn, H. et al. (1982), Z. Phys. B **48**, 109.
34. Leggett, A. J. et al. (1987), Rev. Mod. Phys. **59**, 1; (1995), *ibid* **67**, 725.
35. Weiss, U. (1993) *Quantum Dissipative Systems*, World Scientific.
36. Chudnovski, E. M. (2004), Phys. Rev. Lett. **92**, 120405; (2004), *ibid.* **93**, 158901 and 208901.
37. Feynman, R. P. et al. (1966) *The Feynman Lectures on Physics*, Addison Wesley.
38. Källén, G. (1964) *Elementary Particle Physics*, Addison–Wesley.
39. (a) Carosi, R. et al. (1990), Phys. Lett. B **237**, 303;  
 (b) Alavi–Harati, A. et al. (2003), Phys. Rev. D **67**, 012005;  
 (c) Bertlmann, R. A. et al. (2003), Phys. Rev. A **68**, 012111.
40. Savage, C. M. and Walls, D. F. (1985), Phys. Rev. A **32**, 2316 and 3487.
41. Giulini, D. et al. (Eds) (1996) *Decoherence and the Appearance of a Classical World in Quantum Theory*, Springer.
42. Zurek, W. H. (2002) *Decoherence and the Transition from Quantum to Classical – Revisited*, Los Alamos Science, No. **27**, 2; (quant-physics/0306072).
43. Hornberger, K. and Sipe, J. E. (2003), Phys. Rev. A **68**, 012105.
44. Spohn, H. (1980), Rev. Mod. Phys. **53**, 569.
45. Kimura, G et al. (2001), Phys. Rev. A **63**, 022103.
46. Gerthsen, D. private communication.
47. (a) Kalt, H. *Optical Spectroscopy of Quantum Structures*, in Ref.[1](e);  
 (b) Lyssenko, V. *Coh. Spectr. of SC Nanostruct. and Microcavities*, in Ref.[1](e).
48. (a) Tsitsishvili, E. et al. (2002), Phys. Rev. B **66**, 161405(R);  
 (b) Tsitsishvili, E. et al. (2003), Phys. Rev. B **67**, 205330.
49. Paillard, M. et al. (2001), Phys. Rev. Lett. **86**, 1634.
50. Flissikowski, T. et al. (2001), Phys. Rev. Lett. **86**, 3172.
51. Wheeler, J. A. and Zurek, W. H. (Eds) (1983) *Quantum Theory and Measurement*, Princeton.
52. Zurek, W. H. (2003), Rev. Mod Phys. **75**, 715.
53. Brune, M. et al. (1996), Phys. Rev. Lett. **77**, 4887.